J. Biochem. 127, 687–694 (2000)

Structures of Ovine Corticotropin-Releasing Factor and Its Ala32 Mutant as Studied by CD and NMR Techniques

Kyoung-Seok Ryu,* Byong-Seok Choi,† Seung-Wook Chi,* Seung-Ho Kim,‡ and Hyoungman Kim*,[1]

Department of Biological Sciences and †Department of Chemistry, Korea Advanced Institute of Science and Technology, 373-1 Kusong-dong, Yusong-gu, Taejon 305-701, South Korea; and ‡Protein Function Research Unit, Korea Research Institute of Bioscience and Biotechnology, P.O. Box 115, Yusong, Taejon 305-600, South Korea

Received November 12, 1999; accepted January 6, 2000

The corticotropin-releasing factor (CRF) is a 41–amino acid peptide-amide hormone, which mediates a general stress-response. It has been reported that the substitution of His-32 in the ovine CRF (oCRF) with Ala brings about a 4.5-fold increase in activity [Kornreich *et al.* (1992) *J. Med. Chem.* 35, 1870–76]. Here, we have determined the secondary structure of this Ala-substituted ovine CRF ([Ala32]oCRF) and compare it with that of oCRF using circular dichroism (CD) and NMR techniques in trifluoroethanol (TFE) solution, which is known to stabilize the α-helix formation. In contrast to an earlier report, it was observed the α-helical structure extends to the C-terminus of oCRF. By analyzing the $C_\alpha H$ and NH chemical shifts, the properties of local structures of oCRF were elucidated. The oCRF and [Ala32]oCRF have stable α-helical structures in the middle region, regardless of pH and temperature, and the α-helix initiation regions of these peptides are stabilized as the pH is decreased. However, the [Ala32]oCRF has a more stable α-helical structure than oCRF in the vicinity of the substitution region, and it is thought that this is the cause of the increased activity of [Ala32]oCRF.

Key words: α-helix, CD, chemical shift, corticotropin-releasing factor, NMR, stability.

The corticotropin-releasing factor (CRF) is a peptide hormone consisting of 41 amino acids with an amidated C-terminal end. It is the central hormone that regulates the endocrine, autonomic and behavioral responses to general stress (*1–4*). It belongs to the CRF family, which includes many homologous peptide-amides such as frog sauvagine, fish urotensin I, and mammalian urocortin (*5*). CRF receptors are well known G protein-coupled, seven–transmembrane helices, and signal transmission results in increased intracellular cAMP. CRF receptors occur in two subtypes according to their functions, and they are widely distributed in the body, including in brain, testis, ovary and heart (*6, 7*). It has also been suggested that a 37 kDa CRF-binding protein (CRF-BP) can modulate the overall CRF activity (*8, 9*).

There have been extensive studies on the relationship between the activity and structure of CRF with the ultimate aim of developing more potent drugs. Previous NMR studies in 66% TFE solution showed the structure of h/r (human/rat) CRF to consist of a well-defined α-helix from residue 6 to 36, an extended N-terminus, and a disordered C-terminus (*10*). It is generally accepted that the long α-helical structure is essential for its activity. Kornreich *et al.* studied the general requirements for oCRF activity by substituting of each residue with Ala (*11*). The specific aim of the Ala-substitution was to identify the essential side-chains for hormonal activity among the residues of peptide-hormones, and also to evaluate the importance of the secondary structure, because Ala has only a small CH_3 side-chain and a strong helix-forming propensity (*11, 12*). Among the many Ala-substituted oCRFs, the ones with the substitution in the C-terminal half (residues 20, 22, 25, 26, 29, 32, 33, 34, 39, and 40) increased their activity noticeably, while substitution in the N-termminal half resulted in an appreciable decrease in hormonal activity. In particular, the activity of a mutant oCRF where His32 is replaced by a Ala ([Ala32]oCRF) was 4.5-fold higher than that of the oCRF (*11*). This may mean that, for the rear part of oCRF, its overall structural feature rather than its specific side-chain interaction, is more important for hormonal action.

We selected oCRF and [Ala32]oCRF as model peptide hormones to determine possible local structural differences that may be the cause of their different hormonal activities. For this purpose, we employed CD and NMR techniques, including an analysis of the $C_\alpha H$ and NH chemical shift values, and determined the secondary structures of these peptides in TFE solution. The NMR study of CRF in buffer solution was not performed because of its intermolecular association at the high concentration required for this technique. The TFE solution, although not an realistic system to simulate the actual biological environment, is known to stabilize the α-helical structure of peptide segments (*13*), the inherent helix propensities of sequence homologous peptides being directly related to their α-helix stabilities in TFE solution (*14*). It has also been reported that TFE mimics the amphiphilic environment (*15–17*). It has been well

[1] To whom correspondence should be addressed. Tel: +82-42-869-2615, Fax: +82-42-869-2610, E-mail: hmkim@sorak.kaist.ac.kr

Abbreviations: CD, circular dichroism; oCRF, CSD, chemical shift difference; ovine corticotropin-releasing factor; NMR, nuclear magnetic resonance; MRE, mean residue ellipticity; NOE, nuclear overhauser enhancement; TFE, 2,2,2-trifluoroethanol.

established that the $C_\alpha H$ chemical shift can be used to analyze protein secondary structures (*18–20*), and NH chemical shift can be used to infer the hydrogen-bond length (*21*). Chemical shift also provides information on subtle structural changes in the peptide backbone that are difficult to resolve with a general structure calculation using NOE-constraints (*18*, *22*). Using these techniques, we were able to obtain structural information concerning the segments of oCRF and [Ala32]oCRF. It was found that increased α-helical stability in the C-terminal region of the [Ala32]oCRF including Ala32 is related to the increased activity.

MATERIALS AND METHODS

Synthesis of oCRF and [Ala32]oCRF—These 41 residue peptides, each with a C-terminal amide residue, were synthesized using an automated solid phase peptide synthesizer (Applied Biosystems Model 431A) employing the Fmoc-strategy. First, the C-terminal Fmoc-Ala was coupled to 4-methylbenzhydrylamine (MBHA) resin and then the synthesized peptide was detached from the resin using the general HF-cleavage procedure. This peptide mixture was purified by reversed phase HPLC (C-8) using a water-acetonitrile gradient containing 0.1% trifluoroacetic acid (TFA). The eluents from the HPLC column containing the synthesized peptide hormone were concentrated using a Speed-vac and then lyophilized for long-term storage (~95%). For CD experiments, a shallower water-acetonitrile gradient and a small sample injection were used to achieve high purity (~99%) of the peptides. The purified oCRF and [Ala32]oCRF with molecular weights of 4,670.4 and 4,603.7, respectively, were identified by electron spray ionization-mass spectroscopy (ESI-MS, error range of ±2) and by amino acid composition analysis.

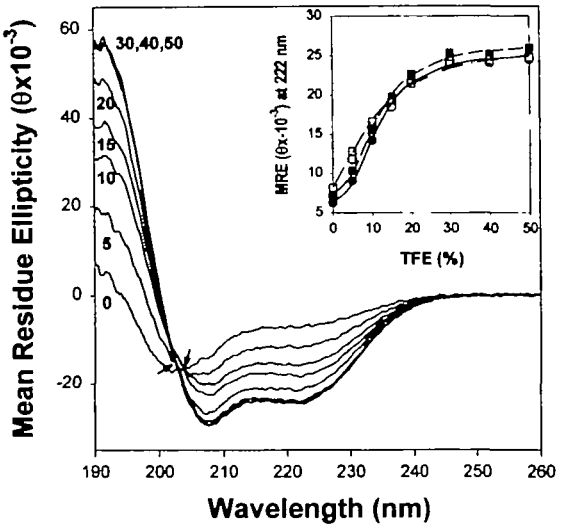

Fig. 1. **Far-UV CD spectra of the oCRF and [Ala32]oCRF.** The concentrations of oCRF and [Ala32]oCRFs were fixed at 20 μM. CD spectra of oCRF were obtained with increasing concentrations (v/v) of TFE (0, 5, 10, 15, 20, 30, 40, 50 indicate volume % of TFE) in 10 mM sodium phosphate buffer at pH 8.0 and 25°C. The arrows indicate two isodichroic points. The inset shows the TFE-titration curves of oCRF and [Ala32]oCRF. The CD spectra of oCRF at pH 3.5 (●) and pH 8.0 (○), and those of [Ala32]oCRF at pH 3.5 (■) and pH 8.0 (□) are shown.

Circular Dichroism (CD) Experiments—CD spectra were obtained with a Jasco J-720 spectropolarimeter using a 0.1 cm path-length quartz cell in a water-circulating thermostat cell holder at 25°C. The concentration of the oCRF stock solution was determined using the value of $[\theta_{\lambda i}]H = [\theta_{\lambda i}]R = -151 \pm 16$, where $[\theta_{\lambda i}]$ is the mean residue ellipticity at the isodichroic point (*23*). The concentration of the [Ala32]oCRF stock solution relative to that of oCRF was determined by fluorescamine assay before and after peptide hydrolysis (*24*). There was no appreciable difference between the concentrations determined before and after peptide hydrolysis, although the sensitivity after hydrolysis was higher. We also obtained the same concentration (within 1% error) of [Ala32]oCRF relative to oCRF using a modified Lowry assay (*25*).

NMR Experiments—Purified oCRF and [Ala32]oCRF were dissolved in 60% (v/v) d_3-TFE solution. The pH was adjusted with a 60% d_3-TFE solution containing either NaOH or HCl at 0.01 and 0.1 N. Proton NMR spectra were recorded with a Bruker DMX 600 spectrometer at 25 and 35°C for the full side-chain assignments. TOCSY spectra of these two peptide hormones were acquired with mixing times of 75 and 100 ms using time-proportional phase incrementation (TPPI) of the first pulse. NOESY spectra were also acquired using TPPI with mixing times of 150 and 250 ms. The NMR data were processed with XWIN-NMR and FELIX 97.2 software.

RESULTS

CD Experiments—Figure 1 shows the CD spectra of oCRF obtained at 25°C. The mean residue ellipticity (MRE) values of oCRF and [Ala32]oCRF at 222 nm as a function of TFE concentration are shown in the inset. It has been reported that oCRF assumes a predominantly helical conformation in TFE solution (*26*). For both oCRF and [Ala32]-oCRF, the general shape of the spectra in the presence of TFE indicates the high α-helical content, while random coil prevails in the absence of TFE. The α-helical contents of oCRF and [Ala32]oCRF increased with increasing TFE concentration and reached a plateau at around 40% TFE. The CD spectra obtained at various TFE concentrations show two isodichroic points close to each other (Fig. 1), one at a TFE concentration of 0% to 15% and the other at a TFE

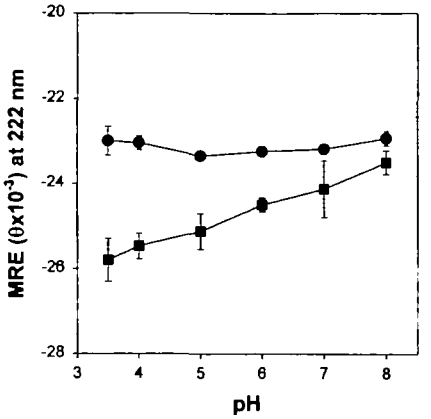

Fig. 2. **Mean residue ellipticities at 222 nm of oCRF (●) and [Ala32]oCRF (■) in 50% TFE solution as a function of pH.**

concentration of 20 to 50%. It has been reported that the isodichroic point not only indicates the presence of a two-state transition, but also provides information about the secondary structure (*23*, *27*). While the isodichroic point at low TFE concentration suggests the existence of a small β-structure population or some multimeric structure of oCRF, the isodichroic point at high TFE concentration is the result of a typical two-state transition between random coin and α-helix (*23*). Therefore, the estimation of the α-helical content at low TFE is uncertain because the oCRF has multimeric structures depending on its concentration in buffer solution (*28*, *29*). However, since a high concentration of TFE induces a monomeric α-helical structure, a precise structural study can be made under these conditions (*13*, *30*). Also, it has been reported that the α-helical propensities of peptides in TFE/water solution can be extrapolated directly to those in buffer solution (*31*). It is of interest that the absolute value of MRE_{222nm} for [Ala32]oCRF is larger than that for oCRF (Fig. 1, inset), the difference rising as the pH is lowered (Fig. 2). The MREs of oCRF at 222 nm did not change as the pH decreased from 8.0 to 3.5, while those of [Ala32]oCRF decreased significantly (Table I). The maximum difference in MRE_{222nm} between oCRF and [Ala32]oCRF at pH 3.5 and in 50% TFE solution corresponds to about 3 more residues of [Ala32]oCRF being involved in the α-helical structure as compared to oCRF (*32*, *33*).

NMR Experiments—The spin-systems of oCRF and [Ala32]oCRFs were identified by TOCSY and NOESY experiments at 25°C and pH 3.5. Since it was difficult to locate the side-chain peaks of Lys23 in the TOCSY spectra obtained at 25°C, we performed the same experiments at 35°C. Extensive peak overlapping was observed in the NH-αH (finger print) region (Fig. 3A), and therefore sequential assignments were made by comparison with the NH-NH region (Fig. 3B). The NMR spectra of [Ala32]oCRF (not shown) are similar to those of oCRF, except in the Ala32 region. The chemical shift values of proton resonance obtained at 35°C and pH 3.5 are given in Tables II and III.

We also performed the same experiment at pH 6.0 and 7.5 for comparison with the CD results. In these cases, sequential assignments were made mainly from the NOESY spectra, because the quality of the TOCSY spectra obtained at these pH values was poor. The 1D spectra of oCRF and [Ala32]oCRF obtained at higher pH showed broader and reduced amide proton peaks, and it is thought that the incomplete magnetization transfer at high pH was the cause of the problem with the TOCSY spectra (*34*). It is possible that the long correlation time resulting from the rigid long helical structure and the faster hydrogen-exchange rate of the amide protons at higher pH caused this incomplete magnetization transfer of TOCSY. Because there was no apparent overall structural change brought about by the pH variation as judged from NOEs, some

TABLE I. **α-Helical contents of oCRF and [Ala32]oCRF.**

	No TFE (at 222 nm)			50% TFE (at 222 nm)		
	MRE × 10^{-3}	Deviation	% (Helix)[a]	MRE × 10^{-3}	Deviation	% (Helix)[a]
wt CRF (pH 3.5)	5.7	0.4	11	23.5	1.2	70
mt CRF (pH 3.5)	7.0	0.4	15	25.8	0.2	77
wt CRF (pH 8.0)	6.3	0.5	13	22.9	0.7	68
mt CRF (pH 8.0)	7.5	0.2	17	23.3	0.9	69

[a]% of α-helix = $(-[\theta]_{MRE} - 2340)/30300 \times 100$.

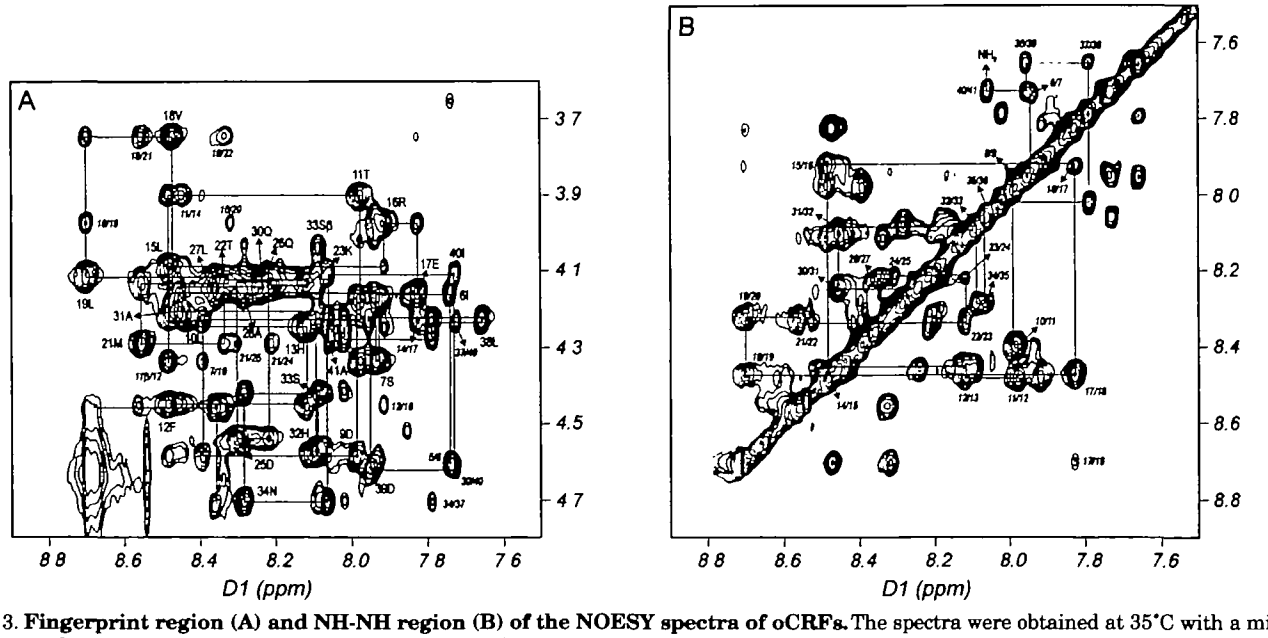

Fig. 3. **Fingerprint region (A) and NH-NH region (B) of the NOESY spectra of oCRFs.** The spectra were obtained at 35°C with a mixing time of 150 ms. Data were acquired using TPPI and the water-signal was suppressed by gradient pulses.

TABLE II. **The chemical shifts of oCRF.**

#		NH	αH	βH	γH	γCH_3	δH	Others
1	S							
2	Q	8.67	4.45	2.19, 2.07	2.41			δNH_2 7.42, 6.63
3	E	8.36	4.72	2.15, 1.97	2.47			
4	P		4.73	2.38, 1.97	2.16, 2.09		3.90, 3.76	
5	P		4.61	2.29	2.13		3.86, 3.65	
6	I	7.73	4.17	1.93	1.64, 1.27	0.98	0.98	
7	S	7.93	4.34	4.02, 3.94				
8	L	7.93	4.18	1.72	1.64		0.96, 0.92	
9	D	7.99	4.58	2.84, 2.72				
10	L	8.38	4.23	1.82	1.78		0.95	
11	T	7.97	3.90	4.33, 4.39		1.22		
12	F	8.48	4.45	3.29, 3.25				ring 7.198, 7.29
13	H	8.12	4.25	3.47				ring 7.375, 8.69
14	L	8.44	4.21	1.92	1.79		0.95	
15	L	8.48	4.09	1.82	1.70		0.91	
16	R	7.92	3.98	1.96, 1.90	1.81, 1.73		3.18, 3.09	εNH 7.33
17	E	7.83	4.16	2.39, 2.29	2.57, 2.49			
18	V	8.47	3.75	2.34	1.13, 0.98			
19	L	8.70	4.12	2.01, 1.88	1.62		0.92	
20	E	8.32	4.13	2.29, 2.22	2.58, 2.50			
21	M	8.55	4.29	2.36, 2.23	2.84, 2.67			
22	T	8.33	4.12	4.46		1.35		
23	K	8.11	4.14	2.03	1.65, 1.52		1.77	ϵCH_2 2.99
24	A	8.20	4.10	1.60				
25	D	8.30	4.54	3.02, 2.91				
26	Q	8.21	4.11	2.35, 2.25	2.64, 2.47			δNH_2 7.24, 6.54
27	L	8.35	4.17	1.94	1.69		0.94	
28	A	8.28	4.16	1.61				
29	Q	8.25	4.14	2.29, 2.27	2.63, 2.48			δNH_2 7.32, 6.57
30	Q	8.23	4.15	2.30, 2.27	2.56, 2.49			δNH_2 7.28, 6.55
31	A	8.45	4.22	1.49				
32	H	8.09	4.57	3.47, 3.33				ring 7.365, 8.54
33	S	8.08	4.42	4.09, 4.04				
34	N	8.28	4.71	2.92				γNH_2 7.34, 6.65
35	R	8.06	4.23	2.00, 1.93	1.78, 1.75		3.26	εNH 7.34
36	K	8.02	4.28	1.94	1.58, 1.53		1.78	ϵCH_2 3.04
37	L	7.79	4.23	1.78	1.70		0.98, 0.92	
38	L	7.65	4.23	1.79	1.65		0.96, 0.90	
39	D	7.95	4.62	2.86				
40	I	7.72	4.11	2.00	1.64, 1.27	0.98	0.91	
41	A	8.05	4.30	1.47				terminal NH_2 7.21, 6.74

overlapping cross peaks in the NOESY spectra obtained at pH 3.5 could be identified using spectra obtained at pH 6.0 and 7.5.

The strong NH-NH connectivities, which are one of the traits of a helical structure, are present from residue 6 to the terminal amide group (Fig. 3B), and many medium range NOEs ($i, i + 3$ and $i, i + 4$) are also shown (Fig. 3A). Although some cross-peaks could not be identified due to extensive overlapping, it is clear that oCRF and [Ala32]-oCRF have long α-helical stretches from residue 5 to the C-terminus. We observed additional medium range NOEs (αH-NH [$i, i + 3$] and αH-βH [$i, i + 3$]) in the C-terminal regions of both oCRF and [Ala32]oCRF, which suggest a possible α-helical structure even at the C-terminal end. The short and medium-range NOE connectivities of the NMR spectra obtained at pH 3.5 and 25°C are summarized in Fig. 4. The $d_{\alpha N}[i, i + 4]$ NOE connectivity of the C-terminus was observed in the case of [Ala32]oCRF but not oCRF. It is possible that the C-terminal end of oCRF is more flexible than that of [Ala32]oCRF.

It was reported that the chemical shifts of α-protons are good indicators of α-helical propensity, because the change in the peptide back-bone from random coil to α-helix results in an up-field shift of α-proton resonance while the α-proton has a downfield shift when the backbone changes to β-strand (*18–20, 35*). We had already observed in CD experiments that oCRF and [Ala32]oCRFs undergo a two-state transition between α-helix and random coil in TFE solution. It is, therefore, possible to compare directly the α-helical stability of oCRF and [Ala32]oCRF using α-proton chemical shifts. The chemical shift differences [CSDs, ($\Delta\delta$) = $\delta_{obs} - \delta_{ref}$] of the $C_\alpha H$ are summarized in Fig. 5. The negative values of the CSDs of [Ala32]oCRF are larger than those of oCRF in the region of residue 32 at pH 3.5 (Fig. 5A). Except for this region, there is no difference in the CSDs between oCRF and [Ala32]oCRF. This suggests that the α-helical structure of the substituted region of [Ala32]-oCRF is more stable than that of the corresponding region of oCRF due to destabilization of the this region in oCRF at low pH, while that of the rest of the peptides is the same at this pH.

Figure 5B shows the pH dependency of the average CSD values from residue 32 to 36 and from residue 20 to 30 of oCRF and [Ala32]oCRF, respectively. Figure 5B-1 shows that the α-helical contents of the middle region of both oCRF and [Ala32]oCRF are about the same and that they are not affected by the change in pH. On the other hand, Fig. 5B-2 indicates that the C-terminal part of oCRF is destabilized as the pH is lowered from 7.5 to 3.5. It is noteworthy that the α-helical content of [Ala32]oCRF in the C-

TABLE III. **The chemical shifts of [Ala32]oCRF.**

#		NH	αH	βH	γH	γCH_3	δH	Others
1	S							
2	Q	8.67	4.46	2.19, 2.06	2.41			δNH_2 7.42, 6.63
3	E	8.33	4.73	2.16, 1.97	2.48			
4	P		4.73	2.39, 1.97	2.15, 2.10		3.89, 3.76	
5	P		4.60	2.29	2.12		3.85, 3.65	
6	I	7.74	4.15	1.94	1.58, 1.27	0.98	0.98	
7	S	7.93	4.33	4.01, 3.95				
8	L	7.90	4.18	1.72	1.64		0.93	
9	D	7.98	4.58	2.86				
10	L	8.40	4.23	1.82	1.78		0.95	
11	T	7.97	3.90	4.32		1.22		
12	F	8.49	4.45	3.29, 3.24				ring 7.20, 7.21
13	H	8.11	4.27	3.47				ring 7.38, 8.71
14	L	8.44	4.22	1.91	1.80		0.95	
15	L	8.49	4.08	1.81	1.71		0.90	
16	R	7.91	3.97	1.95, 1.90	1.72, 1.63		3.18, 3.09	εNH 7.30
17	E	7.82	4.16	2.39, 2.30	2.58, 2.49			
18	V	8.47	3.74	2.34	1.12, 0.97			
19	L	8.70	4.11	2.01, 1.88	1.62		0.91	
20	E	8.31	4.13	2.29, 2.21	2.59, 2.50			
21	M	8.55	4.29	2.35, 2.23	2.83, 2.67			
22	T	8.33	4.10	4.44		1.35		
23	K	8.11	4.15	2.03	1.62		1.77	ϵCH_2 3.00
24	A	8.22	4.12	1.60				
25	D	8.32	4.54	3.06, 2.92				
26	Q	8.21	4.11	2.36, 2.23	2.64, 2.47			δNH_2 7.21, 6.54
27	L	8.34	4.18	1.94	1.69		0.95	
28	A	8.28	4.16	1.61				
29	Q	8.15	4.14	2.27	2.63, 2.45			δNH_2 7.21, 6.53
30	Q	8.24	4.12	2.30	2.54, 2.47			δNH_2 7.26, 6.53
31	A	8.49	4.19	1.57				
32	A	8.18	4.19	1.58				
33	S	8.07	4.30	4.12, 4.03				
34	N	8.18	4.64	2.97, 2.87				γNH_2 7.34, 6.65
35	R	8.03	4.16	2.02	1.80		3.27	εNH 7.31
36	K	7.94	4.24	2.00	1.63, 1.57		1.80	ϵCH_2 3.03
37	L	7.81	4.21	1.84	1.73		0.93	
38	L	7.75	4.21	1.85	1.64		0.98	
39	D	7.97	4.62	2.95, 2.89				
40	I	7.78	4.09	2.02	1.68, 1.28	0.98	0.91	
41	A	8.12	4.15	1.48				terminal NH_2 7.22, 6.74

terminal region appears to be nearly independent of the change in pH. Figure 5B-2 also shows that the CSDs of the C-terminal region vary more than other α-helical parts when the temperature is raised from 25 to 35°C. This means that the C-terminal regions of both oCRF and [Ala32]oCRF are more flexible than the rest of the molecules.

Figure 6 shows the differential $C_\alpha H$ chemical shift values for oCRF and [Ala32]oCRF obtained at pH 3.5 (25 and 35°C) and at pH 6.0 (25°C) relative to the value at pH 7.5 (25°C). Here, a negative difference indicates increased α-helix stability and a positive value shows decreased stability as the pH is lowered. It is clear that the response to the decrease in pH depends on the position in the sequence. In the middle part, the pH change does not affect the α-helical stability, a finding that is in agreement with the results shown in Fig. 5B-1. The pH decrease does not affect the α-helix stability of the [Ala32]oCRF C-terminal segment, but there is a significant decrease in the stability of the oCRF C-terminal area, again, agreeing with the data shown in Fig. 5B-2. In contrast to these results, there is an appreciable increase in the stability in the front part of both oCRF and [Ala32]oCRF as the pH is lowered. In the case of oCRF, the decrease in the stability of the C-terminal region as the pH is lowered is counterbalanced by increased stability in the N-terminal region, resulting in no overall change in stability. In the case of [Ala32]oCRF, an overall net increase in stability can be seen. These observations corroborate the results of CD (Fig. 2).

Figure 7 shows the $\Delta\delta_{NH}$ (δ_{NH} [observed] – δ_{NH} [random coil]) values for oCRF at several pHs. There are no appreciable differences between oCRF and [Ala32]oCRF. NH chemical shift is a typical parameter used to measure the distance between the hydrogen and oxygen in a hydrogen bond in a stable protein structure (*21*). It has been reported that an α-helical peptide with alternating polarity of amino acids gives this type of CSD ($\Delta\delta_{NH}$) variation (*22*, *36*), and the hydrophobic interaction distorts the α-helix into a curve in TFE solution (*37*, *38*). The pattern of the changes observed for the CSD ($\Delta\delta_{NH}$) of residues 21 to 31 is that expected of a curved amphipathic α-helix with repeats of 3 and 4 residues, but it is not clear whether this region interacts with the membrane. Residues 7 to 14 in these peptides show a distinctive zigzag-pattern along the amino acid sequence, and the helical wheel diagram suggests that the region including these residues may interact with the membrane (*28*). The zigzag-pattern of chemical shifts of NH and $C_\alpha H$ shows that the peptide backbone is somehow distorted with a periodicity. It is very interesting that the amplitude of the NH-CSDs of hydrophobic residues in the

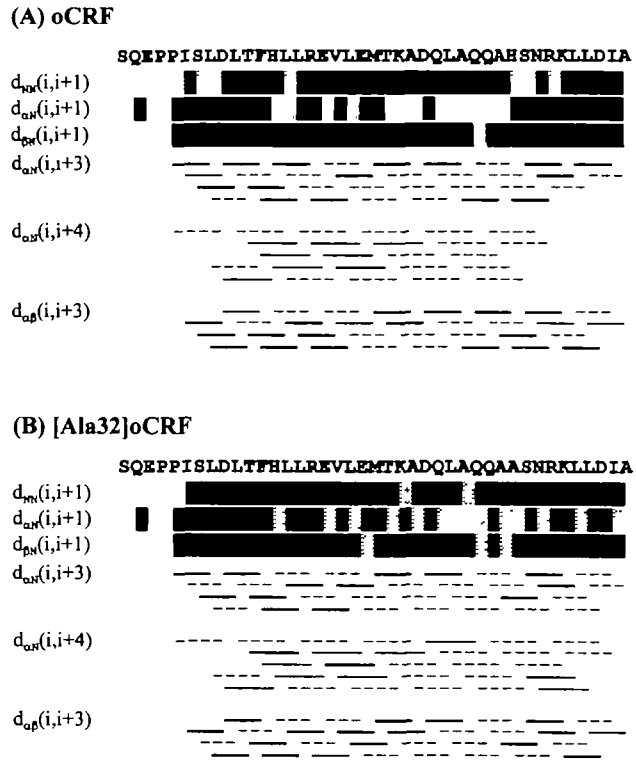

Fig. 4. **Summary of the NOE connectivities of oCRF (A) and [Ala32]oCRF (B).** The medium-range NOE cross-peaks are divided into strong (——), weak (—) and the obscured (——) due to overlap. The short-range NOE cross-peaks are divided into two categories, clear-cut (■) and obscured (▩).

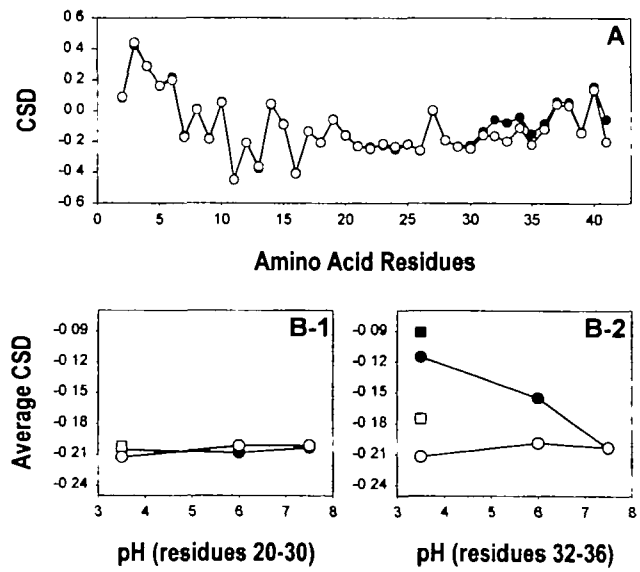

Fig. 5. **The deviation of $C_\alpha H$ chemical shifts from those of random coil.** (A) Chemical shift differences of oCRF (●) and [Ala32]-oCRF (○) at 35°C, pH 3.5. The average values of CSDs from residues 20 to 30 (B-1) and those from residues 32 to 36 (B-2) at 25°C (●: oCRF, ○: [Ala32]oCRF) and at 35°C (■: oCRF, □: [Ala32]oCRF) are also shown.

periodic region (residues 8, 10, 12, 14, 15) became lower when the pH was increased from 3.5 into 7.5. This characteristic pattern of NH-CSD may be caused by reduced hydrogen bond lengths between i and $i + 4$ residues in this segment due to interaction between the hydrophobic side chains brought together by hydrogen bonds, producing a more stable α-helical structure as the pH was decreased. We also observed that the NOE peak between Pro5 βH and Leu8 NH became weak as the pH was increased (data not shown).

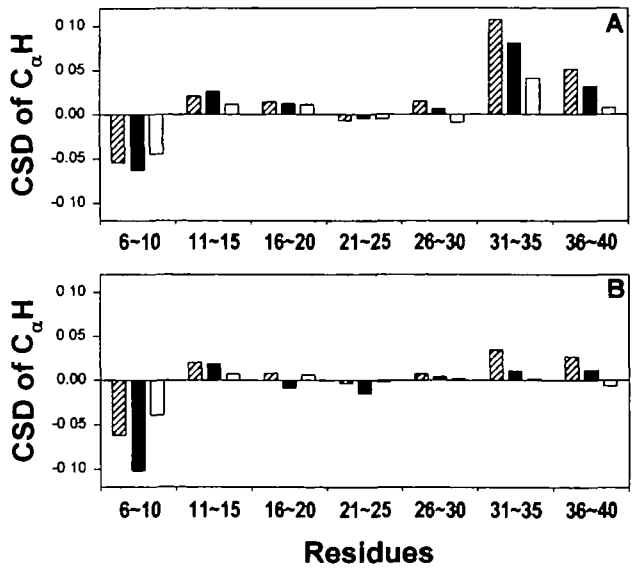

Fig. 6. **The relative $C_\alpha H$ chemical shifts of oCRF and [Ala32]-oCRF.** The chemical shift values of $C_\alpha H$ obtained at pH 3.5 and 35°C (cross-hatched), pH 3.5 and 25°C (black), and pH 6.0 and 25°C (white) are subtracted with those of at pH 7.5 and 25°C for oCRF (A) and [Ala32]oCRF (B).

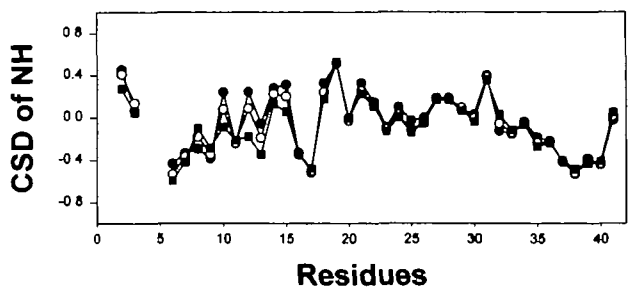

Fig. 7. **The NH chemical shift differences of oCRF.** The chemical shift differences ($\Delta\delta_{NH}$: $\delta_{observed} - \delta_{random\ coil}$) of oCRF at 25°C and pH 3.4 (●), at 25°C and pH 6.0 (○), and at 25°C and pH 7.5 (■) are plotted against residue number.

DISCUSSION

The primary aim of this investigation was to elucidate the cause of the increased potency of [Ala32]oCRF over native oCRF by comparing their structures in TFE solution. Even though TFE solution is not a realistic model system in which to simulate a real biological system, such as the ligand-binding site of receptors, it is a convenient and effective system because of its amphiphilic characteristics. Also, the α-helix forming region of homologous peptides can be deduced by study in TFE solution. The CD results show a

slightly higher α-helical content for [Ala32]oCRF as compared to oCRF at neutral pH and the gap increased with decreasing pH. On the other hand, the NOEs obtained by 2D NMR suggested that the same general regions, from residue 5 to the C-terminus, in both oCRF and [Ala2]oCRF have α-helix propensities. Chemical shift analysis based on NOE data is a simple yet powerful method to analyze the properties of the local structure in a long α-helix. Analysis of the chemical shift values of $C_\alpha H$ and NH revealed that the different α-helix segments in these peptides have different stabilities. The α-helical structure of oCRF obtained in 50% TFE solution could be divided into three parts according to stability. The main structural difference between oCRF and [Ala32]oCRF lies in the C-terminal region containing the substitution site at low pH. While the α-helix of [Ala32]oCRF in this region remains independent of pH change, the same region in oCRF is destabilized at low pH.

The N-terminal section of the α-helix is assumed to form an amphipathic α-helix (*28*), and also has an unusual sequence motif including repeats of hydrophilic and lipophilic amino acids (HL-repeat). According to the results of $C_\alpha H$ CSDs, the α-helix initiation region is stabilized as the pH is decreased (Fig. 6). It is possible that a favorable interaction between His13 and Asp9 causes this stabilization, although we could not find any supporting NOE peaks between the side chains of these residues. The stabilization of the N-terminal region of the α-helix with decreasing pH is also supported by NH CSDs (Fig. 7), which show that the amplitude of the zigzag pattern increases as the pH is decreased. It has been reported that the N-terminal region plays important roles in receptor activation (*5*, *39*) and it is possible also that the pH-dependent α-helical stability of the N-terminus may play a role in receptor activation through interaction with the membrane.

The mid section of both peptides form stable α-helices at both temperatures and at every pH studied here. The C-terminal α-helix section of both peptides appears to be rather flexible, and this part of oCRF is less favorable for a stable α-helix at pH below 6.0 than that of [Ala32]oCRF. The unfavorable ionic interaction of His32 (pK_a = 6.04) with Arg35 and Lys36 in oCRF may be the cause of this. It is likely that the 4.5-fold increase in the activity of [Ala32]oCRF over oCRF arises from the stabilization of the α-helix in the C-terminal region including residue 32. It has been reported that the removal of the C-terminal amide results in a 1,000-fold decrease in activity (*1*). It is possible that the C-terminal amide participates in a direct interaction with the receptor. However, it is also possible that the C-terminal negative charge that is produced by deamidation may be the cause of the reduced helical stability in this terminal region by opposing the helix-dipole (*40–42*).

There is some quantitative discrepancy in the α-helical content when the results of $C_\alpha H$ CSDs are compared with the CD results. The extent of the downfield shifts of oCRF in the vicinity of residue 32 is larger than that of upfield shifts in the α-helix initiation region as the pH is decreased from 7.5 to 3.5. On the other hand, the CD results showed that the α-helical content of oCRF does not change appreciably with changing pH. It is probable that the $C_\alpha H$ upfield shift of the α-helix initiation region is different from those of the common α-helix region in the vicinity of residue 32. The α-helix initiation regions of oCRF and [Ala32]-oCRF have distinctive sequence motifs (HL-repeats), and the $C_\alpha H$ CSDs of this region vary differently from those of common α-helices.

It was recently suggested that the binding motif of CRF is the helix-turn-helix with the turn centered around residues 31–32, based on computer modeling with an Ac-Ala_{13}-NH_2 scaffold including the cyclization of i and i + 3 residues (*39*). However, it is possible that the active conformation of these antagonists is still an α-helix–like structures *in vivo* (*43*), or the increased rigidity induced by cyclization is important for activity. It is of interest to note that the antagonist with double-cyclization between residues 20 and 23, and 30 and 33 shows a lower activity compared to the antagonist with only one cyclization (*39*). It is clear from the above results that the CRF binds to its receptor in a more complicated induced fit fashion.

Although it is possible that the destabilization of C-terminal region of oCRF at lower pH may have some bearing on the differential activity of this peptide and [Ala32]-oCRF, this is by no means certain because the difference in α-helix stability occurs only at lower pH. It is possible, however, that the pH close to the surface of bilayers containing negatively charged phospholipids is more acidic than the bulk aqueous phase (*44*, *45*).

REFERENCES

1. Vale, W., Spiess, J., Rivier, C., and Rivier, J. (1981) Characterizaion of a 41-residue ovine hypothalamic peptide that stimulates secretion of corticotropin and β-endorphin. *Science* **213**, 1394–1397
2. Richard, D. (1992) Involvement of corticotropin-releasing factor in the control of food intake and energy expenditure. *Ann. N. Y. Acad. Sci.* 155–172
3. Menzaghi, F., Heinrichs, S.C., Pich, E.M., Weiss, F., and Koob, G.F. (1992) The role of limbic and hypothalamic corticotropin-releasing factor in behavioral respinses to stress. *Ann. N. Y. Acad. Sci.* 142–154
4. Dufau, M.L., Tinajero, J.C., and Fabbri, A. (1993) Corticotropin-releasing factor: an antireproductive hormone of the testis. *FASEB J.* **7**, 299–307
5. Rivier, J., Rivier, C., and Vale, W. (1984) Synthetic competitive antagonists of corticotropin-releasing factor: Effect on ACTH secretion in the rat. *Science* **224**, 889–891
6. Chalmers, D.T., Lovenbergand, T.W., and De Souza, E.B. (1995) Localization of novel corticotropin-releasing factor receptor (CRF2) mRNA expression to specific subcortical nuclei in rat brain: comparison with CRF1 receptor mRNA expression. *J. Neurosci.* **15**, 6340–6350
7. Lovenberg, T.W., Chalmers, D.T., Liu, C., and De Souza, E.B. (1995) CRF2 alpha and CRF2 beta receptor mRNAs are differentially distributed between the rat central nervous system and peripheral tissues. *Endocrinology* **136**, 4139–4142
8. Woods, R.J., Kennedy, K.M., Gibbins, J.M., Behan, D., Vale, W., and Lowry, P.J. (1994) Corticotropin-releasing factor binding protein dimerizes after association with ligand. *Endocrinology* **135**, 768–773
9. Lowry, P.J., Koerber, S.C., Woods, R.J., Baigent, S., Sutton, S., Behan, D.P., Vale, W., and Rivier, J. (1996) Nature of ligand affinity and dimerization of corticotropin-releasing factor-binding protein may be detected by circular dichroism. *J. Endocrinol.* **16**, 39–44
10. Romier, C., Bernassau, J.-M., Cambillau, C., and Drabon, H. (1993) Solution structure of human corticotropin releasing factor by ^1H NMR and distance geometry with restrained dynamics. *Protein Eng.* **6**, 149–156
11. Kornreich, W.D., Galyean, R., Hernandez, J.-F., Craig, A.G., Donaldson, C.J., Yamamoto, G., Rivier, C., Vale, W., and Rivier,

J. (1992) Alanine series of ovine corticotropin releasing factor (oCRF): A structure-activity relationship study. *J. Med. Chem.* **35**, 1870–1876
12. O'Neil, K.T. and DeGrado, W.F. (1990) A thermodynamic scale for the helix-forming tendencies of the commonly occurring amino acids. *Science* **250**, 646–651
13. Sonnichsen, F.D., Van Eyk, J.E., Hodges, R.S., and Sykes, B.D. (1992) Effect of trifluoroethanol on protein secondary structure: An NMR and CD study using a synthetic actin peptide. *Biochemistry* **31**, 8790–8798
14. Walgers, R., Lee, T.C., and Cammers-Goodwin, A. (1998) An indirect chaotropic mechanism for the stabilization of helix conformation of peptides is aqueous trifluoroethanol and hexafluoro-2-propanol. *J. Am. Chem. Soc.* **120**, 5073–5079
15. Jasanoff, A. and Fercht, A.R. (1994) Quantitative determination of helical protensities from trifluoroethanol titration curves. *Biochemistry* **33**, 2129–2135
16. Motta, A., Pastore, A., Goud, N.A., and Castiglione Morelli, M.A. (1991) Solution conformation of salmon calcitonin in sodium dodecyl sulfate micelles as determined by two-dimensional NMR and distance geometry calculations. *Biochemistry* **30**, 10444–10450
17. Mukhopadhyay, K. and Basak, S. (1998) Conformation induction in melanotropic peptides by trifluoroethanol: fluorescence and circular dichroism study. *Biophys. Chem.* **74**, 175–186
18. Wishart, D.S. and Sykes, B.D. (1994) Chemical shifts as a tool for structure determination in *Methods in Enzymology* (James, T.L. and Oppenheimer, N.J., eds.) Vol. 239, pp. 363–439, Academic Press, New York
19. Wishart, S., Sykes, B.D., and Richards, F.M. (1992) The chemical shift index: A fast and simple method for the assignment of protein secondary structure through NMR spectroscopy. *Biochemistry* **31**, 1647–1651
20. Weber, P.L., Brown, S.C., and Mueller, L. (1987) Sequential ^{1}H NMR assignments and secondary structure identification of human ubiquitin. *Biochemistry* **26**, 7282–7290
21. Wagner, G., Pardi, A., and Wuthrich, K. (1983) Hydrogen bond lengths and ^{1}H NMR chemical shifts in proteins. *J. Am. Chem. Soc.* **105**, 5948–5949
22. Blanco, F.J., Herranz, J., González, C., Jiménez, M.A., Rico, M., Santoro, J., and Nieto, J.L. (1992) NMR chemical shifts: A tool to characterize distortions of peptide and protein helices. *J. Am. Chem. Soc.* **114**, 9676–9677
23. Holtzer, M.E. and Holtzer, A. (1992) α-Helix to random coil transition: Determination of peptide concentration from the CD at the isodichroic point. *Biopolymers* **32**, 1675–1677
24. Udenfriend, S., Stein, S., Bohlen, P., and Dairman, W. (1972) Fluorescamine: A reagent for assay of amino acids, peptides, proteins, and primary amines in the picomole range. *Science* **178**, 871–872
25. Peterson, G.L. (1983) Determination of total protein in *Methods in Enzymology* (Hirs, C.H.W. and Timasheff, S.N., eds.) Vol. 91, pp. 95–121, Academic Press, New York
26. Pallai, P.V., Mabilia, M., Goodman, M., Vale, W., and Rivier, J. (1983) Structural homology of corticotropin-releasing factor, sauvagine, and urotensin I: circular dichroism and prediction studies. *Proc. Natl. Acad. Sci. USA* **80**, 6770–6774
27. Merutka, G. and Stellwagen, E. (1989) Analysis of peptides for helical prediction. *Biochemistry* **28**, 352–357
28. Lau, S.H., Rivier, J., Vale, W., Kaiser, E.T., and Kézdy, F.J. (1983) Surface properties of an amphiphilic peptide hormone and of its analog: Corticotropin-releasing factor and sauvagine. *Proc. Natl. Acad. Sci. USA* **80**, 7070–7074
29. Morii, H., Uedaira, H., Ishimura, M., Kidokoro, S.-I., Kokubu, T., and Ohashi, S. (1997) Special folding pathway to tetramer only through the micelle state of the corticotropin-releasing factor. *Biochemistry* **36**, 15538–15545
30. Zhou, N.E., Zhu, B.-Y., Kay, C.M., and Hodges, R.S. (1992) The two-stranded α-helical coiled-coil is an ideal model for studying protein stability and subunit interactions. *Biopolymers* **32**, 419–426
31. Luo, P. and Baldwin, R.L. (1997) Mechanism of helix induction by trifluoroethanol: A framework for extrapolating the helix-forming properties of peptides from trifluoroethanol/water mixtures back to water. *Biochemistry* **36**, 8413–8421
32. Chen, Y.H. and Yang, J.T. (1971) A new approach to the calculation of secondary structure of globular proteins by optical rotatory dispersion and circular dichroism. *Biochem. Biophys. Res. Commun.* **44**, 1285–1291
33. Chen, Y.H., Yang, J.T., and Chau, K.H. (1974) Determination of the helix and β form of proteins in aqueous solution by circular dichroism. *Biochemistry* **13**, 3350–3359
34. Kay, L.E., Ikura, M., and Bax, A.D. (1991) The design and optimization of complex NMR experiments. Application to a triple-resonance pulse scheme correlating Hα, NH, and ^{15}N chemical shifts in ^{15}N-^{13}C-labeled proteins. *J. Magn. Reson.* **91**, 84–92
35. Hill, J.M., Oomen, C.J., Miranda, L.P., Binghan, J.-P., Alewood, P.F., and Craik, D.J. (1998) Three-dimensional solution structure of α-conotoxin MII by NMR spectroscopy: Effects of solution environment on helicity. *Biochemistry* **37**, 15621–15630
36. Hoyt, D.W. and Gierasch, L.M. (1991) Hydrophobic content and lipid interactions of wild-type and mutant OmpA signal peptides correlate with their in vivo function. *Biochemistry* **30**, 10155–10163
37. Lazo, N.D. and Downing, D.T. (1997) Circular dichroism of model peptides emulating the amphipathic alpha-helical regions of intermediate filaments. *Biochemistry* **36**, 2559–2565
38. Zhou, N.E., Zhu, B.-Y., Sykes, B.D., and Hodges, R.S. (1992) Relationship between amide proton chemical shifts and hydrogen bonding in amphipathic α-helical peptides. *J. Am. Chem. Soc.* **114**, 4320–4326
39. Koerber, S.C., Gulyas, J., Lahrichi, S.L., Corrigan, A., Craig, A.G., Rivier, C., Vale, W., and Rivier, J. (1998) Constrained corticotropin-releasing factor (CRF) agonists and antagonists with $i - (i + 3)$ Glu-Xaa-DXbb-Lys bridges. *J. Med. Chem.* **41**, 5002–5011
40. Armstrong, K.M. and Baldwin, R.L. (1993) Charged histidine affects alpha-helix stability at all positions in the helix by interacting with the backbone charges. *Proc. Natl. Acad. Sci. USA* **90**, 11337–11340
41. Zimm, B.H. and Bragg, J.K. (1959) Theroy of the phase transition between helix and random coil in polypeptide chains. *J. Chem. Phys.* **31**, 526–535
42. Lifson, S. and Roig, A. (1961) On the theory of helix-coil transition in polypeptides. *J. Chem. Phys.* **34**, 1963–1974
43. Gulyas, J., Rivier, C., Perrin, M., Koerber, S.C., Sutton, S., Corringan, A., Lahrichi, S.L., Craig, A.G., Vale, W., and Rivier, J. (1995) Potent, structurally constrained agonists and competitive antagonists of corticotropin-releasing factor. *Proc. Natl. Acad. Sci. USA* **92**, 10575–10579
44. van der Goot, F.G., Gonzalez-Manas, J.M., Lakey, J.H., and Pattus, F. (1991) A molten-globule membrane-insertion intermediate of the pore-forming domain of colicin A. *Nature* **354**, 408–410
45. Fernandez, M.S. (1981) Determination of surface potential in liposomes. *Biochim. Biophys. Acta* **6**, 23–26